Biomechanical constraints on the feedforward regulation of endpoint stiffness

Xiao Hu, Wendy M. Murray and Eric J. Perreault

J Neurophysiol 108:2083-2091, 2012. First published 25 July 2012;
doi: 10.1152/jn.00330.2012

Journal of Neurophysiology publishes original articles on the function of the nervous system. It is published 24 times a year (twice monthly) by the American Physiological Society, 9650 Rockville Pike, Bethesda MD 20814-3991. . ESSN: 1522-1598. Visit our website at http://www.the-aps.org/.

J Neurophysiol 108: 2083–2091, 2012.
First published July 25, 2012; doi:10.1152/jn.00330.2012.

Biomechanical constraints on the feedforward regulation of endpoint stiffness

Xiao Hu,[1,2] Wendy M. Murray,[1,2,3,4] and Eric J. Perreault[1,2,3]

[1]*Department of Biomedical Engineering, Northwestern University, Evanston, Illinois;* [2]*Sensory Motor Performance Program, Rehabilitation Institute of Chicago, Chicago, Illinois;* [3]*Department of Physical Medicine and Rehabilitation, Northwestern University, Chicago, Illinois; and* [4]*Research Service, Edward Hines, Jr. VA Hospital, Hines, Illinois*

Submitted 20 April 2012; accepted in final form 20 July 2012

Hu X, Murray WM, Perreault EJ. Biomechanical constraints on the feedforward regulation of endpoint stiffness. *J Neurophysiol* 108: 2083–2091, 2012. First published July 25, 2012; doi:10.1152/jn.00330.2012.—Although many daily tasks tend to destabilize arm posture, it is still possible to have stable interactions with the environment by regulating the multijoint mechanics of the arm in a task-appropriate manner. For postural tasks, this regulation involves the appropriate control of endpoint stiffness, which represents the stiffness of the arm at the hand. Although experimental studies have been used to evaluate endpoint stiffness control, including the orientation of maximal stiffness, the underlying neural strategies remain unknown. Specifically, the relative importance of feedforward and feedback mechanisms has yet to be determined due to the difficulty separately identifying the contributions of these mechanisms in human experiments. This study used a previously validated three-dimensional musculoskeletal model of the arm to quantify the degree to which the orientation of maximal endpoint stiffness could be changed using only steady-state muscle activations, used to represent feedforward motor commands. Our hypothesis was that the feedforward control of endpoint stiffness orientation would be significantly constrained by the biomechanical properties of the musculoskeletal system. Our results supported this hypothesis, demonstrating substantial biomechanical constraints on the ability to regulate endpoint stiffness throughout the workspace. The ability to regulate stiffness orientation was further constrained by additional task requirements, such as the need to support the arm against gravity or exert forces on the environment. Together, these results bound the degree to which slowly varying feedforward motor commands can be used to regulate the orientation of maximum arm stiffness and provide a context for better understanding conditions in which feedback control may be needed.

endpoint stiffness; musculoskeletal model; short-range stiffness; arm impedance; postural stability

HUMANS USE THEIR ARMS AND hands to interact with and manipulate a variety of objects in different environments. Although many daily tasks tend to destabilize the arm (Rancourt and Hogan 2001), it is still possible to have stable interactions with the environment by regulating arm mechanics in a task-appropriate manner. Although the central nervous system (CNS) is responsible for the regulation of arm mechanics, we do not yet have a complete understanding of the limits on this regulation and the mechanisms by which it occurs. During unconstrained tasks, posture selection plays a critical role in the regulation of limb mechanics (Milner 2002; Mussa-Ivaldi et al. 1985; Trumbower et al. 2009). When posture is constrained, however, the nervous system can regulate mechanics only by changing muscle activation through feedforward mechanisms such as cocontraction or feedback mechanisms including the many types of stretch-evoked reflexes (Franklin and Milner 2003; Gomi and Osu 1998; Krutky et al. 2010; Perreault et al. 2002). Although both feedforward mechanisms, which we define as steady-state levels of muscle activation, and feedback mechanisms, defined as responses evoked by a postural disturbance, are able to alter arm mechanics, the relative efficacy of these two mechanisms has yet to be determined. This is important for understanding not only unimpaired motor control, but also how impairments influencing feedforward and feedback control, such as stroke, cerebral palsy, and Parkinson's disease, alter the ability to regulate arm mechanics in a functionally appropriate manner.

The static mechanics of the arm are often quantified by estimates of endpoint stiffness, the steady-state relationship between perturbations applied at the hand and the forces generated in response. Endpoint stiffness is directional, resisting perturbations in certain directions more strongly than in others. The major axis of the stiffness ellipse indicates the orientation of the maximum endpoint stiffness, a convenient measure of how the contributions from all active muscles contribute to directional nature of endpoint stiffness. Changing muscle activations to reorient the direction of maximum stiffness is one method for tuning arm mechanics to the requirements of a specific task, and quantifying this ability has often been used to assess the ability of the nervous system to regulate arm mechanics in a task-appropriate manner (Burdet et al. 2001; Franklin et al. 2007; Lacquaniti et al. 1993; Perreault et al. 2002). During the maintenance of posture, the ability to alter stiffness orientation is quite limited (Darainy et al. 2004; Gomi and Osu 1998; Perreault et al. 2002) relative to that reported during movement (Burdet et al. 2001; Franklin et al. 2003, 2007). It has been argued that the level of control over stiffness orientation that has been observed during movement results at least partially from regulation of the feedforward motor commands (Burdet et al. 2001; Franklin et al. 2003). However, it is not clear why similar regulation would not be effective during the maintenance of posture.

During the maintenance of posture, feedforward control of endpoint stiffness orientation could be constrained by neural or biomechanical factors or a combination of both. Neural constraints include the inability to activate muscles independently. For example, the activation levels of biarticular muscles crossing the shoulder and elbow often covary with those of the monoarticular elbow muscles (Gribble and Ostry 1998; Osu and Gomi 1999). If the organization of the nervous system specifies that these muscles are most easily activated together, the ability to regulate stiffness orientation could be reduced. Alternatively, biomechanical constraints associated with the geometric properties of the musculoskeletal system and the

Address for reprint requests and other correspondence: X. Hu, Dept. of Biomedical Engineering, Northwestern Univ., 345 E. Superior St., Chicago, IL 60611 (e-mail: xiaohu2011@u.northwestern.edu).

stiffness properties of its muscles may also limit the ability to control stiffness orientation, independent from any neural constraints (Valero-Cuevas 2005). For example, stiffening a limb through cocontraction requires the coordinated activity of many muscles so as to achieve the desired stiffness while also balancing the torques throughout the limb. Because muscles have three-dimensional (3-D) moment arms and can cross more than one joint, and few muscles are pure antagonists, even simple cocontraction tasks typically involve many muscles to resolve the biomechanical constraints imposed by the design of the musculoskeletal system (Yamazaki et al. 2003). It is challenging to discriminate between neural and biomechanical constraints using only experimental studies involving human subjects, since the two systems work in concert during most functional tasks. Musculoskeletal modeling provides a complementary approach that can be used to isolate the biomechanical constraints on motor behavior. Such models have proven useful for investigating the control of endpoint stiffness (Flash and Mussa-Ivaldi 1990; Tee et al. 2004, 2010), but none of these previous studies was designed specifically to explore how the architecture of the musculoskeletal system influences the ability to control stiffness orientation across different tasks, and none incorporated the 3-D anatomy required to meet that objective.

The purpose of the present study was to investigate how the biomechanical properties of the musculoskeletal system constrain the ability to regulate endpoint stiffness orientation through feedforward control of muscle activation. This investigation was accomplished using a realistic musculoskeletal model of the human arm coupled with a scalable model of muscle stiffness, which we previously demonstrated produces robust and accurate estimates of endpoint stiffness (Hu et al. 2011). This simulation approach allows us to identify how the biomechanical design of the upper limb constrains the control of stiffness orientation in isolation from the constraints that may arise from neural structures. We hypothesized that the feedforward control over endpoint stiffness orientation would be significantly constrained by the biomechanical properties of the musculoskeletal system. Furthermore, we hypothesized that the effects of these constraints would increase during functional tasks that place additional demands on the neuromuscular system such as the exertion of voluntary forces.

METHODS

Modeling. The musculoskeletal model used in this study was reported previously and shown to characterize the endpoint stiffness of the human arm over a wide range of arm postures and endpoint forces (Hu et al. 2011). In summary, the model has 2 components: a muscle model characterizing muscle-tendon short-range stiffness (Cui et al. 2008) and a realistic musculoskeletal model of the human arm adapted from Holzbaur et al. (2005) that incorporates 4 kinematic degrees of freedom (shoulder flexion/extension, abduction/adduction, and internal/external rotation and elbow flexion/extension) and 37 arm muscles (or muscle compartments; Fig. 1*A*).

The muscle-tendon model (Cui et al. 2008) assumes that the muscle-tendon short-range stiffness, K, can be approximated by two elements in series (*Eq. 1*): a tendon with stiffness, K^t, and a muscle with stiffness, K^m.

$$K = \frac{K^m K^t}{(K^m + K^t)} \tag{1}$$

The tendon stiffness was approximated by the generic, dimensionless force-strain curve proposed by Zajac (1989). The muscle stiffness was scaled by muscle force according to *Eq. 2*, in which F^m is the current force generated by the muscle, l_0^m is the optimal muscle fiber length at maximum activation, and γ is a dimensionless constant (23.4) describing the scaling of the short-range stiffness with muscle force (Cui et al. 2008).

$$K^m = \frac{\gamma F^m}{l_0^m} \tag{2}$$

The musculoskeletal model of the arm adapted from Holzbaur et al. (2005) as described in Hu et al. (2011) was used to obtain parameter values for optimal muscle fiber lengths, maximum isometric muscle forces, tendon slack lengths, and muscle moment arms, as needed for the simulations. Based on these physiological parameters, muscle short-range stiffness was calculated from *Eqs. 1* and *2* and transformed to endpoint coordinates by the Jacobians relating joint coordinates to muscle coordinates (J) and endpoint coordinates (G). This resulted in a model-based estimate of endpoint stiffness, K^e.

$$K^j = J^T \vec{K} J + \frac{\partial J^T}{\partial \theta} \vec{F}^m + K^j_{pass} \tag{3}$$

$$K^e = (G^{-1})^T \left[K^j - \frac{\partial G^T}{\partial \theta} F^{end} \right] G^{-1} \tag{4}$$

This transformation is shown in *Eqs. 3* and *4*, in which $\vec{K}$ is the matrix describing muscle short-range stiffness, K^j is the matrix describing

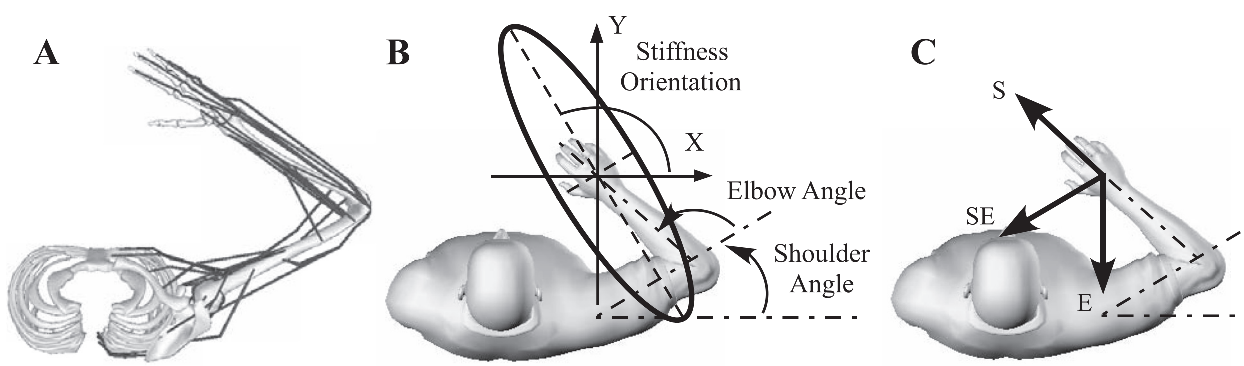

Fig. 1. Model simulations. *A*: musculoskeletal model of the human arm with 37 arm muscles (or muscle compartments) used in this study. *B*: coordinate systems for measuring arm posture and endpoint stiffness orientation. The latter was defined as the angle between *x*-axis and the major axis of the ellipse. The posture shown in this figure was used in *simulation experiments 1, 2,* and *4*. *C*: the directions of the endpoint forces applied in *simulation experiment 2*. These resulted in net torques about shoulder (S), elbow (E), or a combination of both (SE).

joint stiffness, θ is the joint angle vector, and $\vec{F}^m$ and F^{end} are the muscle force and endpoint force vectors, respectively. The passive joint stiffness matrix, K^j_{pass}, was taken directly from experimental data (Perreault et al. 2001). The transformation defined by *Eq. 4* was restricted in the horizontal plane, only considering shoulder flexion/extension and elbow flexion/extension. The orientation of endpoint stiffness was calculated using the method described by Gomi and Osu (1998).

In contrast to the mapping from individual muscle stiffnesses to endpoint stiffness provided by implementing both *Eqs. 3* and *4*, one previous approach to modeling endpoint stiffness has been to consider only the relationship between joint stiffness and endpoint stiffness described by *Eq. 4* (Flash and Mussa-Ivaldi 1990; Tee et al. 2004). To compare the results of our 3-D model with the approach considering only joint stiffness, we implemented a planar, two-joint model with a joint stiffness matrix given by *Eq. 5*. The parameters in this matrix describe the joint stiffnesses attributed to the lumped *1*) monoarticular shoulder muscles (K^s), *2*) monoarticular elbow muscles (K^e), and *3*) biarticular muscles (K^{bi}). In *Eq. 5*, r is the ratio of the muscle moment arms at the shoulder and at the elbow for the biarticular muscles. If r = 1, the moment arms at the shoulder and elbow are assumed to be equal for these muscles. This form of the joint stiffness matrix allowed us to investigate the critical role of biarticular muscle moment arms on the controllability of endpoint stiffness orientation (Tee 2003).

$$K^j = \begin{bmatrix} K^s + \mathrm{r}K^{bi} & K^{bi} \\ K^{bi} & \dfrac{K^{bi}}{\mathrm{r}} + K^e \end{bmatrix} \tag{5}$$

The maximum values of $K^s + \mathrm{r}K^{bi}$, $\dfrac{K^{bi}}{\mathrm{r}} + K^e$, and K^{bi} were obtained from the maximum corresponding values across all tested arm postures reported by Flash and Mussa-Ivaldi (1990).

Model-based estimation of stiffness orientation control. The achievable range of endpoint stiffness orientations was assessed via simulation to address four distinct questions, described in detail below. In each case, a constrained optimization algorithm solved for the muscle activations that generated the desired endpoint stiffness properties. The first three simulations considered the range of stiffness orientations that could be achieved. Optimization was used to determine the maximum clockwise and counterclockwise changes in the orientation of endpoint stiffness. The controllable range of stiffness orientations for a given simulation was then defined as the difference between these two values. The final simulation considered the maximum stiffness magnitude that could be achieved in all directions, without consideration for the orientation of the corresponding endpoint stiffness. All optimizations were performed using an active-set algorithm, as implemented in MATLAB. A wide range of randomly selected initial conditions was used to ensure that a global minimum was reached; results were found to be robust with respect to the selected initial condition.

In all simulations, the arm was constrained to act in the horizontal plane, allowing for comparison with the majority of previous experimental and simulation studies. Three of the simulated conditions (*simulation experiments 1*, *2*, and *4*) considered a single arm posture with the elbow flexed to 117° and the shoulder flexed to 26° (Fig. 1*B*). These values were chosen to reflect postures at which endpoint stiffness orientation has been shown to be most changeable (Gomi and Osu 1998) and to match approximately prior experimental data collected by our group (Perreault et al. 2002). Arm posture was allowed to vary in the third set of simulations.

Simulation experiment 1: control of endpoint stiffness orientation. In our first set of simulations, we examined the degree to which the orientation of endpoint stiffness can be controlled by changing muscle activation patterns in postural conditions where there are no forces exerted on the environment. To do so, we calculated the coordination patterns that resulted in zero net moments about the shoulder and elbow and compared the results of these simulations to others performed under a range of constraints that reflect different experimental paradigms described in the literature. For example, the postural studies reported by Gomi and Osu (1998) and Perreault et al. (2002) required postures and muscle activations to be maintained for durations that would elicit fatigue at maximal activation levels. To assess how requiring a sustained level of muscle activity for a relatively long period of time might affect stiffness orientation control, we compared results of simulations in which the maximum activation for each muscle was restricted to levels ranging between 10 and 100%. Similarly, previous experimental studies evaluating the control of endpoint stiffness have differed regarding whether they have required the subjects to support the weight of the arm against gravity (Franklin et al. 2007; Perreault et al. 2002). To evaluate how requiring voluntary support against gravity influences the control of stiffness orientation, we compared results of simulations in which the influence of gravity was excluded (i.e., 0 net moments about the shoulder and elbow) and simulations in which the voluntary shoulder abduction and axial rotation torques required to counter gravity were produced by the muscle activation pattern calculated via the optimization algorithm. The magnitudes of the torques required to counter gravity were estimated assuming typical arm segment masses for an average American adult male (86 kg) (Ogden et al. 2004).

Simulation experiment 2: influence of voluntary force generation on the control of stiffness orientation. The second set of simulations considered postural tasks in which voluntary forces are exerted against the environment, conditions that have been previously shown to reduce the ability to control stiffness orientation volitionally (Perreault et al. 2002). We performed simulations that compared the influence of endpoint forces that result from only net shoulder torques, from only net elbow torques, and from combinations of shoulder and elbow torques (Fig. 1*C*) (Gomi and Osu 1998; Mussa-Ivaldi and Hogan 1991). For each of these force directions, the volitional force requirement was scaled from 0 to 100% of the maximum achievable force in each direction. Gravitational forces were not considered. Inward directions were selected since these directions, which require use of the shoulder and elbow flexors, tend to be much stronger than the opposite, outward directions. As such, they are expected to have a greater influence on the ability to regulate stiffness orientation since the generation of these inward forces (when scaled to the maximum achievable force) requires more of the total muscle activation that is available, leaving less activation that can be used to control stiffness orientation independently.

Simulation experiment 3: influence of arm posture on the control of stiffness orientation. The first two simulations considered only a single arm posture, approximately matched to experimental conditions in which the volitional control of stiffness orientation was shown to be largest. The third set of simulations allowed posture to vary systematically to determine how stiffness control varies throughout the workspace. Specifically, the shoulder angle was varied from −30 to 90° by increments of 10°, and the elbow angle was varied from 0 to 130°, using increments of 10° from 0 to 110° and using increments of 2° from 110 to 130°. Smaller increments were used for the elbow angle from 110 to 130° because the controllable range of stiffness orientation varied more quickly for these values. For these simulations, endpoint force was constrained to zero, and gravitational torques were not considered. Achievable muscle activation levels were set to 100% of the maximum.

The same procedure was repeated using the simplified model (*Eq. 5*) to evaluate the influence of arm posture on the ability to control stiffness orientation. This was achieved by optimizing the values of K^s, K^e, and K^{bi} with the constraint that all values remain within the previously reported experimental estimates (Flash and Mussa-Ivaldi 1990). Since the ratio of the biarticular muscle moment arms at the elbow and shoulder is known to influence the controllability of stiffness orientation, this simulation was repeated for two different moment arm ratios. First, a moment arm ratio of 1 (r = 1) was considered, as used in previous simulation studies (Flash and Mussa-Ivaldi 1990). Next, we considered a ratio based on our detailed musculoskeletal model. Specifically, we averaged the ratios of the three biarticular muscles included in our model (biceps long and short heads and triceps long head) at each specific arm posture.

Simulation experiment 4: ability to maximize stiffness in a specific direction. Although the previous simulations focused on the ability to regulate the orientation of maximum stiffness, it is important to remember that this may not be the most effective way to reject perturbations in a particular direction. Rather, due to the constraints on the biomechanical system, the maximum stiffness that can be achieved in any particular direction may not correspond to the stiffness that can be achieved when the endpoint stiffness ellipse is oriented in that same direction. To evaluate this possibility, we also optimized stiffness magnitude along directions ranging from 0 to 180° (5° increments) in the horizontal plane without consideration for stiffness orientation. In these simulations, there were no constraints on the amount of muscle activation (within the physiological range) or other forces that needed to be compensated. Only the posture used for *simulation experiments 1* and *2* was considered.

Sensitivity analysis. Monte Carlo analyses were conducted to evaluate the sensitivity of the estimated endpoint stiffness control range to parameters in our musculoskeletal model (Hughes and An 1997; Santos and Valero-Cuevas 2006). Our previous work (Hu et al. 2011) showed that model-based estimates of stiffness orientation were most sensitive to small changes in muscle moment arms and joint angles. Hence, only these model parameters were considered in the present study. We used Monte Carlo simulations to estimate the influence of these model parameters on the achievable range of endpoint stiffness orientations. Parameters were considered independent and allowed to vary simultaneously. Each parameter was randomly selected from a normal distribution with a mean defined by our model and a standard deviation derived from the plausible range over which these parameters could be expected to vary across the population. The standard deviation of the muscle moment arms was set to 20% of the nominal parameter values (Murray et al. 2002). The standard deviation for the joint angles was set to 4°, the accuracy with which angles can be measured with a manual goniometer (Fish and Wingate 1985; Grohmann 1983). Sensitivity analyses were performed only for the first simulation experiment. Two hundred simulations were performed for each of the conditions simulated in this experiment; these conditions corresponded to the evaluated constraints on joint torque and muscle activation. The results of each Monte Carlo simulation were summarized by the standard deviation of achievable range of endpoint stiffness orientations.

RESULTS

Simulation experiment 1: control of endpoint stiffness orientation. The range of achievable endpoint stiffness orientations was biomechanically constrained at the fixed arm posture used in our first two simulated experiments. In our least constrained condition at this posture (i.e., no forces exerted on the environment, maximum activation level is 100%, and muscles do not have to support the weight of the arm against gravity), stiffness orientation could be varied over a range of 93°, from 49 to 142° (Fig. 2). Relative to the orientation of passive endpoint stiffness, varying muscle activation patterns could alter the orientation of maximum stiffness predominantly in the clockwise direction (72°), which has been shown to result largely from activation of the elbow muscles (Gomi and Osu 1998; Perreault et al. 2002). At the extreme clockwise orientation, endpoint stiffness became nearly isotropic.

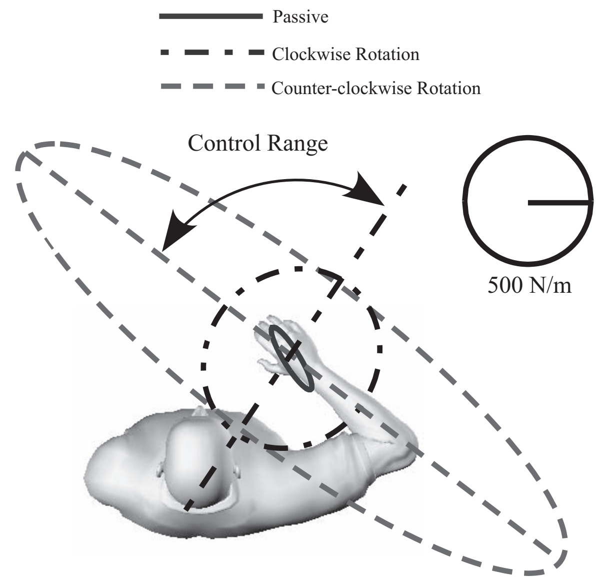

Fig. 2. Control of endpoint stiffness orientation at a fixed arm posture. The only constraint in these simulations was that the net torque about the shoulder and elbow remained at 0 for all selected levels of steady-state muscle activation. The small solid ellipse shows the passive stiffness simulated in the model. The dashed and dot-dashed ellipses illustrate the extent of the achievable orientations in the counterclockwise and clockwise directions, respectively.

The range of achievable endpoint stiffness orientations was substantially reduced when muscle activation was restricted to levels that could be sustained for significant periods of time. There was a monotonic decrease in the achievable control range as the maximum allowable muscle force was decreased (Fig. 3). At 30% of maximum muscle force, a value that typically can be sustained for ≥2 min (Avin et al. 2010), the orientation of endpoint stiffness could be changed by 19° in the counterclockwise direction and 50° in the clockwise direction, for a total range of 69°. At 10% maximum muscle force, this range was reduced to only 52°.

Requiring the muscle activity to support the arm against gravity further reduced the control range (Fig. 3). This result occurred because the gravitational constraint limited the range of muscle activations that could be used only to control endpoint stiffness orientation. Specifically, requiring gravitational support limited the control range when muscle forces were restricted to remain below 90% of the maximum activation. With the additional restriction of supporting the arm against gravity, the control range was only 41° at 30% of maximum muscle force. Achievable solutions were not obtained for values of muscle activation <30%. It is notable that these most restrictive simulations approximate those used in our previous experimental studies (Perreault et al. 2002) in which subjects were required to support the arm against gravity and in which each experimental trial lasted for ~2 min or longer. In those experimental studies, the measured control range across all subjects was 30 ± 8° (Fig. 3), similar but still smaller than the comparable simulation results. The remaining differences may reflect neural constraints not included in our model.

The model-based estimates of the control range of endpoint stiffness orientation were robust to small changes of joint angles and muscle moment arms (Fig. 3, error bars). When both joint angles and muscle moment arms were varied simultaneously, the maximum variation of the control range was 23°. This maximal variation was observed for the least con-

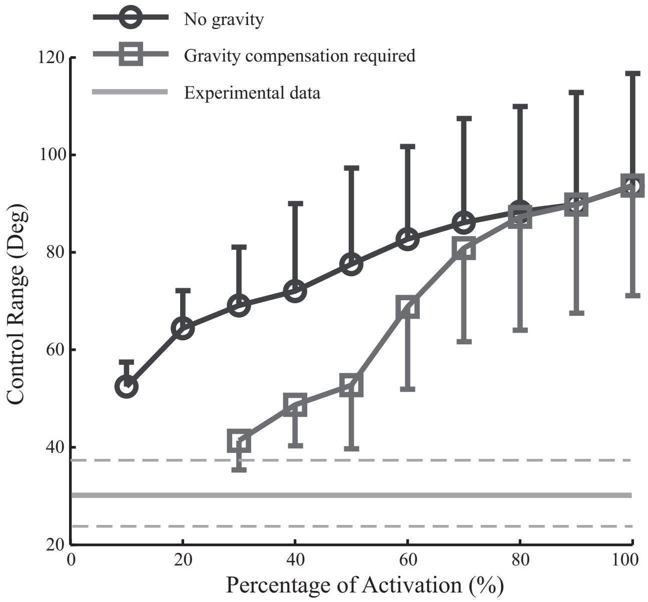

Fig. 3. Influence of maximal allowable muscle activation on the achievable range of endpoint stiffness orientations. Curves with circles are the simulations in which gravity was not considered. Curves with squares correspond to simulations in which muscle activity was required to support the arm against gravity. Error bars (SD) illustrate the results of the Monte Carlo simulations used to evaluate model sensitivity to variations in muscle moment arms and measured joint angles. The experimental data and the associated standard deviations (dashed lines) are taken from Perreault et al. (2002) for comparison. Deg, degrees.

strained simulations, during which muscle forces were allowed to vary over the entire physiological range. At 30% of maximum muscle force, the sensitivity to these parameter fluctuations reduced to 12° in the absence of gravity and to 6° when gravitational constraints were considered.

Simulation experiment 2: influence of voluntary force generation on the control of stiffness orientation. The ability to control stiffness orientation changed dramatically when the model was also required to exert steady-state endpoint forces. In general, the range of stiffness orientations decreased with increasing volitional force (Fig. 4). When exerting forces that required activation of the shoulder muscles or the shoulder and elbow muscles, there was a monotonic decrease in the range of orientations that could be achieved as the magnitude of the endpoint force increased. In contrast, there was an initial increase in the range of orientations that could be achieved when exerting forces that required only activation of the elbow muscles; beyond ~10% of the maximum achievable endpoint force in this direction, the orientation range decreased monotonically as it did for the other tested force directions. This initial increase in the range of achievable orientations occurred because the endpoint forces required by the simulated task resulted in a small clockwise shift of stiffness orientation, thereby biasing the range.

Simulation experiment 3: influence of arm posture on the control of stiffness orientation. The control of endpoint stiffness orientation was biomechanically constrained throughout most of the reachable workspace. These constraints were most dramatic at distal arm postures (Fig. 5*A*). For >85% of the reachable area, the range of achievable orientations was <60°. Changes in elbow angle had the most dramatic effect on the controllability of stiffness orientation. When the elbow was flexed more than ~124°, full control of stiffness orientation could be achieved. This high degree of elbow flexion positioned the hand very close to the trunk and could be reached only in a small portion of the simulated workspace. In contrast to the elbow angle, changes in shoulder angle had only a modest influence on the controllability of stiffness orientation.

The simplified musculoskeletal models had similar posture-dependent patterns of stiffness orientation control as our more detailed model but larger areas of the workspace in which full control could be achieved. For the first simple simulation, equal moment arms were assumed for all muscles. Under this assumption, full control of stiffness orientation could be obtained for all tested elbow flexion angles >100°; changes in shoulder angle had no influence on the ability to control stiffness orientation (Fig. 5*B*). Tee (2003) demonstrated the importance of the moment arm ratio between the muscle crossing the elbow and shoulder when considering the orientation of endpoint stiffness. To simulate more realistic conditions than equal moment arms, we matched the moment arm ratio of the shoulder and elbow muscles (details in METHODS) to that in our more detailed model. Under these conditions (Fig. 5*C*), an even more restricted control of endpoint stiffness was observed.

Simulation experiment 4: ability to maximize stiffness in a specific direction. Preferentially orienting the direction of maximum stiffness is not necessarily the most effective way to increase endpoint stiffness in a particular direction during postural tasks. This was assessed by maximizing the magnitude of endpoint stiffness in each direction without regard to the orientation of the net stiffness ellipse. Using this approach, we found a large variation in the maximum stiffness magnitude that could be achieved in any given direction of interest (cf. Fig. 6*A*, magnitudes range from approximately 2,500 to 8,000 N/m). For the specific direction in which the peak stiffness magnitude was achieved (cf. Fig. 6*B*, peak stiffness is ~8,000 N/m at ~110°), the orientation of the stiffness ellipse was aligned with the direction of interest. That is, for a direction of 110°, the maximum stiffness magnitude was achieved when the net endpoint stiffness ellipse was oriented in this same direction. This was not the case in most other directions (cf. Fig. 6*B*, comparing our results with the dashed line having sloping of 1). When stiffness magnitude was optimized in each direction, stiffness orientation varied

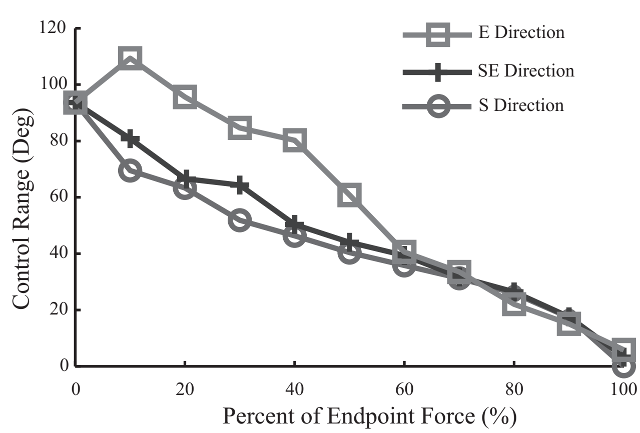

Fig. 4. Influence of endpoint force on the control of endpoint stiffness orientation. Simulations were performed for endpoint forces that required activation on only the elbow muscles (E task), the shoulder muscles (S task), or the shoulder and elbow muscles (SE task), as shown in Fig. 1*C*. Endpoint force magnitudes were scaled from 0 to 100% of the maximum possible force in each direction.

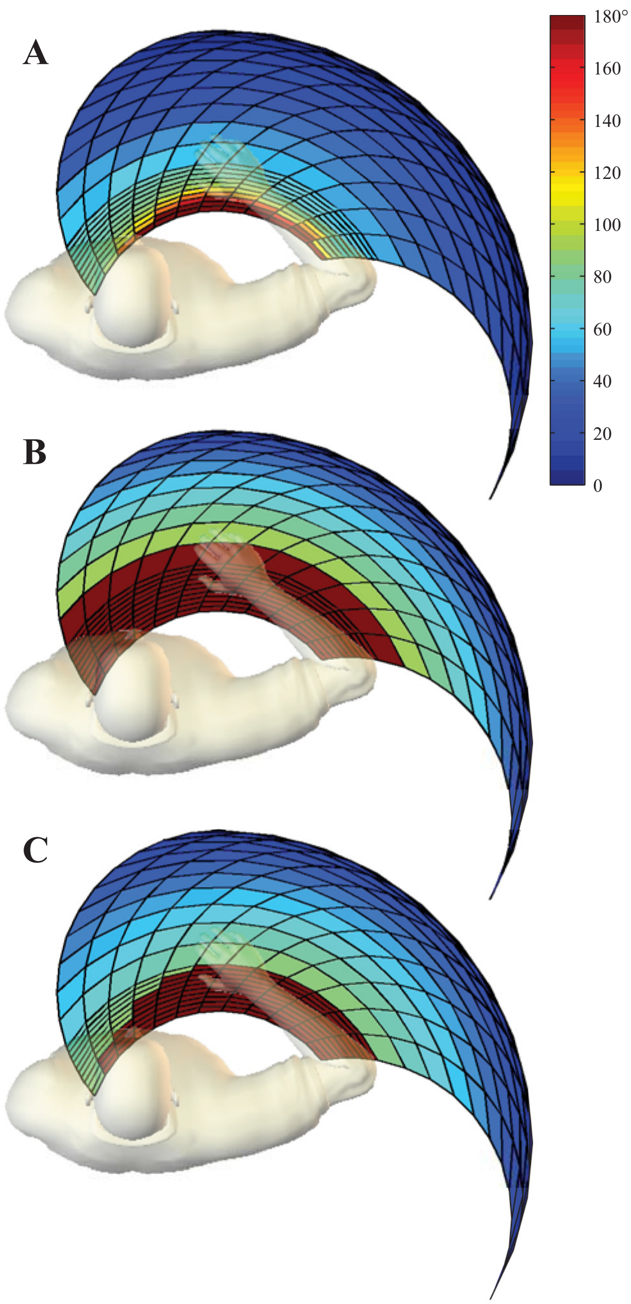

Fig. 5. Posture-dependent range of endpoint stiffness orientations. *A*: the control range predicted by the full musculoskeletal model. *B*: the control range predicted by the simplified model assuming equal moment arms of biarticular muscles at the shoulder and at the elbow. *C*: the control range predicted by the simplified model with the ratio of biarticular muscle moment arms matched to those used in our model. In all simulations, shoulder horizontal flexion was varied from −30 to 90° in increments of 10°; elbow flexion angle was varied from 0 to 110° in increments of 10° and from 110 to 130° in increments of 2°.

over a range of 88–133°, well within achievable range of orientations determined in *simulation experiment 1*. The shape of the endpoint stiffness ellipse, representing the ratio of the stiffness magnitudes in the shortest and longest directions, was relatively constant for the posture tested (Fig. 6*C*).

DISCUSSION

This study examined the degree to which the biomechanical design of the human arm constrains the ability to regulate endpoint stiffness. Specifically, we examined variations in the orientation of maximal stiffness that can be obtained using constant muscle activations as relevant to the feedforward regulation of arm posture. The control of endpoint stiffness orientation was assessed using a previously validated 3-D musculoskeletal model of the human arm that incorporates scalable models of muscle short-range stiffness (Hu et al. 2011). By using such a model, it was possible to assess the extent to which endpoint stiffness could be controlled if there were no constraints on how the human nervous system could independently activate the muscles of the arm. Our results demonstrated substantial biomechanical constraints on the ability to regulate endpoint stiffness orientation throughout the workspace even when the arm was not required to generate any net torque about the elbow and shoulder. The ability to regulate stiffness was further constrained by additional task requirements such as the need to support the arm against gravity or exert forces on the environment. Finally, we demonstrated that although preferentially orienting the direction of maximum stiffness was not the most effective means for increasing stiffness in a particular direction, the range of orientations of the stiffness ellipses that result from simply maximizing stiffness magnitude in a specific direction fell well within the controllable range we predicted. Together, these results bound the degree to which slow feedforward motor commands can be used to regulate the orientation of maximum arm stiffness and

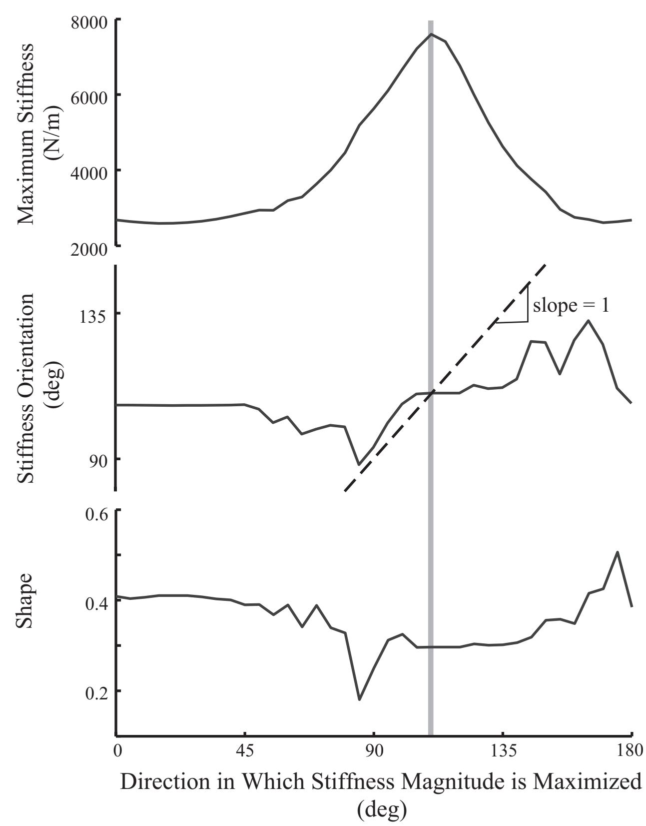

Fig. 6. Endpoint stiffness resulting from maximizing the stiffness magnitude in specific directions throughout the horizontal plane. *A*: stiffness magnitude resulting from the optimization process. *B*: the orientation of the net endpoint stiffness ellipse resulting from the optimization. The dashed line represents the orientations that would be expected if stiffness in each direction was maximized by preferentially orienting the direction of maximum endpoint stiffness. *C*: the shape of the endpoint stiffness ellipse resulting from this optimization.

provide a context for understanding the most effective means by which stiffness can be increased in a specific direction and for identifying conditions in which feedback control may be needed.

Biomechanical constraints on endpoint stiffness control. Our results demonstrate that arm posture has a dramatic effect on the ability to regulate endpoint stiffness orientation. These findings help to explain the influence of arm posture on the ability to control unstable loads (Milner 2002) and the discovery that subjects self-select postures that match the orientation of maximal arm stiffness to the stability requirements of the task being performed (Trumbower et al. 2009). The influence of posture on endpoint stiffness has been documented in numerous experiments, including passive (Mussa-Ivaldi et al. 1985) and active (Gomi and Osu 1998; Perreault et al. 2001) conditions. Gomi and Osu (1998) evaluated the influence of posture on the ability to control stiffness orientation and found results broadly similar to those from our simulations. Specifically, they showed that a full control of stiffness orientation could not be achieved at any of the tested postures and that the greatest degree of control occurred as the most proximal hand postures. Our results suggest that many of these posture-dependent changes can be attributed to the geometry of the musculoskeletal system and the mechanical constraints associated with maintaining a specific posture. In ~85% of the evaluated workspace, the range of achievable stiffness orientations was <60°. Only in regions very close to the body was the control of stiffness orientation not constrained by the biomechanical characteristics of the neuromuscular system. In addition to greater regulation of stiffness orientation, the more proximal hand postures also tend to exhibit a more isotropic endpoint stiffness, which may have advantages over the distal postures when encountering unexpected loads (Milner 2002).

The control of stiffness orientation was further constrained by any ongoing muscle activity required to complete a specific task. For example, restricting the maximum muscle force to levels that could be sustained during longer postural tasks, voluntarily supporting the weight of the arm against gravity, and exerting forces against objects in the environment all reduced the range of stiffness orientations that could be achieved. These results are due to at least two factors. First, the muscle activation required for the task sets a baseline stiffness that biases the orientation of stiffness that can be achieved by further increases in muscle activation. Second, an ongoing task limits the degree to which muscle activation can be further increased before fatigue or strength limitations are reached. Similar findings have been observed in experimental studies (Perreault et al. 2002), although it was not possible to determine from the experimental data if these task-related limitations in stiffness control were due to constraints on whether the nervous system can activate muscles independently or on the biomechanical constraints of the task. Our simulation results suggest that biomechanical constraints play an important role in the reduced control range of stiffness orientation that has been observed in experimental studies. In addition, our findings indicate that protocol differences related to the tasks being performed by a subject may contribute to some of the discrepancies noted in the literature, regarding the control of stiffness orientation. The most dramatic differences in the control of stiffness orientation have been noted to exist between postural (Darainy et al. 2004; Gomi and Osu 1998; Perreault et al. 2002; Selen et al. 2009) and movement (Burdet et al. 2001; Franklin et al. 2007) studies. Many of the postural studies require sustained muscle activity that is not a requirement in the movement protocols, where transient activations are sufficient to achieve the task goals. Hence, we expect that the constraints on stiffness control associated with restrictions on activation level (see Fig. 3) would be lesser in movement tasks relative to postural tasks, although the magnitude of the reduction in control range we observed when restricting activation level suggests this factor is unlikely to account for all of the differences reported in these studies (Darainy et al. 2007). In general, our simulation results illustrate that any aspects of an experimental protocol that require substantial muscle activation (e.g., voluntarily supporting the weight of the arm against gravity) or limit the maximum activation that can be achieved are likely to reduce the ability to control stiffness orientation.

Changing the orientation of maximum stiffness is not the only means by which endpoint stiffness can be regulated to compensate for external perturbations of posture. We were able to demonstrate that the maximum stiffness that can be achieved in any direction is often obtained using cocontraction patterns that do not precisely orient the net endpoint stiffness of the arm toward the direction of interest. These results are similar to results demonstrating that force targets in a specific direction are often preferentially achieved by generating a net force vector that is not coaligned with the target (Pan et al. 2005). Our results are also consistent with those of Selen et al. (2009), who showed that in an unstable force production task, subjects generally did not perfectly align the orientation of maximum stiffness with the direction of the environmental instability when the posture of the arm was constrained. In addition to the tradeoff between stability and neuromotor noise suggested by Selen et al. (2009), our results also suggest that there often can be a biomechanical advantage to choosing stiffness orientations that are not aligned to the task goals.

Comparison with other models of endpoint stiffness. Other studies have also modeled the control range of stiffness orientations that could be achievable but have produced some conflicting results. Tee et al. (2004) demonstrated slightly larger control ranges than the maximum reported here when considering similar postures. However, that work was not explicitly conducted to consider muscle properties, the need for balancing torques created by individual muscles, or how the geometric properties of the musculoskeletal system beyond changes in joint angles influence the control of stiffness orientation. Darainy et al. (2004) concluded that control of stiffness orientation was constrained, reporting a number similar to our lowest estimates (~35°). Their model, however, required elbow and shoulder muscles to be activated synergistically, thereby enforcing a simulated neural constraint. In contrast, our study focused only on the effects of biomechanical constraints, allowing any possible patterns of muscle coactivation, which could have led to a larger control range than those reported by Darainy et al. (2004). Finally, recent work by Tee et al. (2010) expanded on their own earlier study to consider the activation of individual muscles and predicted that endpoint stiffness could be oriented arbitrarily within the same horizontal plane considered in our work. The main goal of the Tee et al. (2010) study was to examine an algorithm for stiffness adaptation, and some of the modeling choices were made to achieve that goal. Most important for the control of stiffness orientation was the selection of the moment arms of the biarticular muscles crossing the elbow and shoulder. These were selected "to produce feedback modification mainly in the double joint muscles" (Tee et al. 2010). Previous work by Tee (2003) nicely demonstrated that the ability to control endpoint stiffness orientation is strongly dependent on the ratio of shoulder-to-elbow moment arms for the biarticular muscles. The ratio of 1.3 used in the 2010 paper does indeed provide full control of stiffness orientation, as was intended, but seems to fall outside of the range of physiological values reported in the literature. Although we are unaware of comprehensive anatomic studies explicitly documenting muscle moment arms at the shoulder and elbow in the same specimens, comparing moment arms between studies that focused on the shoulder (Itoi et al. 2008) and elbow (Murray et al. 2002) joints indicates that the moment arms at the shoulder are less than those at the elbow for the biarticular heads of the biceps and triceps. This is partially supported by the results of Dhaliwal and Milner (2003), who used electrical stimulation of the biceps to estimate the relative moment arms for this muscle based on the measured torques about the shoulder and elbow. They reported an average shoulder-to-elbow moment arm ratio of 0.75 ± 0.19. Because our model calculates angle-dependent moment arms that were validated relative to experimental data collected from cadaveric specimens (Holzbaur et al. 2005), it can be used to compute this moment arm ratio throughout the simulated range of motion. Throughout the evaluated workspace, the average ratio was 0.74 ± 0.26, substantially less than that used by Tee et al. (2010) but comparable with that reported by Dhaliwal and Milner (2003). We incorporated these posture-dependent moment arm ratios into the simplified model described by *Eq. 5* and demonstrated that this approach also predicts a substantial limitation on the control of endpoint stiffness orientation throughout most of the reachable workspace when anatomically appropriate moment arm ratios are considered for the biarticular muscles. It is worth noting that although the biarticular moment arm ratio is important for determining the control of stiffness orientation, arm postures also play a crucial role. Our model-based estimate of the moment arm ratio ranged from 0.27 to 1.66 (Fig. 5*C*) compared with constant ratio 1 used in Fig. 5*B*, but this difference had a substantial impact on the control of stiffness orientation only for the more flexed shoulder and elbow postures.

In contrast to previous models of endpoint stiffness, the proposed model considers the 3-D geometry of the arm and the full complement of muscles that can influence stiffness control. This increased complexity has advantages and disadvantages. The obvious disadvantage is the model complexity for both simulation and interpretation of results. The advantages are related to a more accurate characterization of the musculoskeletal mechanics, such as the moment arm ratios discussed above, and an understanding of how those mechanics influence stiffness control. A more complex model with realistic muscle properties and geometric characteristics also provides a tool for estimating critical parameters that then can be incorporated into simpler models as demonstrated in Fig. 5*C*. Finally, the 3-D characteristics of our model provide a means for assessing task-dependent stiffness control in a manner that would be difficult when using simplified representations of arm stiffness. Because of the complex geometry of the limb, muscles rarely act in exact opposition. Hence, using cocontraction to stabilize a joint typically involves sets of agonists and antagonists that cannot easily be represented in models that incorporate joints with only a single degree of freedom or simplified moment arm representations. Rather, the 3-D geometry of the arm is likely to enforce synergistic patterns of muscle activation (Berniker et al. 2009; Kutch and Valero-Cuevas 2011), thereby further constraining the ability to control stiffness independently from the task being performed.

Implications for the neural control of stiffness regulation. Although our results emphasize the importance of biomechanical constraints, they do not rule out the existence of additional neural constraints on the control of endpoint stiffness. Indeed, the postural experiments most similar to our simulation studies demonstrated an achievable range of stiffness orientations that tended to be smaller than that predicted by the simulation results (Darainy et al. 2004; Gomi and Osu 1998; Perreault et al. 2002). These differences may result from neural constraints such as the coupled action of biarticular and elbow muscles (Gribble and Ostry 1998; Osu and Gomi 1999). Such constraints could easily be incorporated into the optimization algorithm to assess their influence on stiffness control, although that was not the purpose of the present study. The results we have presented provide a baseline for determining the maximum degree to which feedforward control of muscle activation can be used to regulate endpoint stiffness in the absence of additional neural constraints.

There have been a number of experimental studies demonstrating a control of endpoint stiffness orientation well beyond that shown to be possible in our simulations (Burdet et al. 2001; Franklin et al. 2007; Kadiallah et al. 2011). All of these experimental studies differed from our simulations in one important respect, which is that they considered stiffness control during movement rather than the postural conditions considered in our simulations. Since the endpoint of the limb is not in static equilibrium during movement, the muscle activation patterns available to regulate stiffness orientation can be somewhat different from those required for the postural conditions simulated in our study, possibly allowing more flexible control of stiffness orientation. Alternatively, although the mechanisms are unclear, it has been suggested that stiffness during movement is lower than would be expected based on postural studies (Bennett et al. 1992; Popescu et al. 2003), which could have an effect on the ability to regulate endpoint stiffness by changing the baseline stiffness required to complete the task. Finally, the results from these movement studies may suggest involvement from feedback pathways not considered in our model (Franklin et al. 2007; Krutky et al. 2010; Mutha et al. 2008) or other mechanisms that contribute to the apparent fundamental differences between the control of posture and movement (Darainy et al. 2007). Nonetheless, the model we have presented provides an important tool for assessing the limits of feedforward control and for assessing conditions in which feedback or other mechanisms are necessary to explain experimental findings.

ACKNOWLEDGMENTS

We thank Etienne Burdet for insightful comments and additional data related to the model presented in Tee et al. (2010) and Elise Walker for the assistance with manuscript preparation.

Portions of this work have been presented previously in abstract form (Hu et al. 2010a,b).

GRANTS

This work was supported by National Institutes of Health Grants R01-NS-053813 and R01-EB-011615 and the National Science Foundation program in Cyber-Physical Systems.

DISCLOSURES

No conflicts of interest, financial or otherwise, are declared by the author(s).

AUTHOR CONTRIBUTIONS

Conception and design of the simulations were by X.H., W.M.M., and E.J.P. Simulations were performed by X.H. Analysis and interpretation of data were done by X.H., W.M.M., and E.J.P. Drafting the article was done by X.H. Revising the article critically for important intellectual content was done by X.H., W.M.M., and E.J.P. All authors approved the final version of the manuscript.

REFERENCES

Avin KG, Naughton MR, Ford BW, Moore HE, Monitto-Webber MN, Stark AM, Gentile AJ, Law LA. Sex differences in fatigue resistance are muscle group dependent. *Med Sci Sports Exerc* 42: 1943–1950, 2010.

Bennett D, Hollerbach J, Xu Y, Hunter I. Time-varying stiffness of human elbow joint during cyclic voluntary movement. *Exp Brain Res* 88: 433–442, 1992.

Berniker M, Jarc A, Bizzi E, Tresch MC. Simplified and effective motor control based on muscle synergies to exploit musculoskeletal dynamics. *Proc Natl Acad Sci USA* 106: 7601–7606, 2009.

Burdet E, Osu R, Franklin DW, Milner TE, Kawato M. The central nervous system stabilizes unstable dynamics by learning optimal impedance. *Nature* 414: 446–449, 2001.

Cui L, Perreault EJ, Maas H, Sandercock TG. Modeling short-range stiffness of feline lower hindlimb muscles. *J Biomech* 41: 1945–1952, 2008.

Darainy M, Malfait N, Gribble PL, Towhidkhah F, Ostry DJ. Learning to control arm stiffness under static conditions. *J Neurophysiol* 92: 3344–3350, 2004.

Darainy M, Towhidkhah F, Ostry DJ. Control of hand impedance under static conditions and during reaching movement. *J Neurophysiol* 97: 2676–2685, 2007.

Dhaliwal H, Milner T. A method for determining the moment arm ratio of biarticular muscles in vivo using electrical stimulation. *Engineering in Medicine and Biology Society, 2003. Proceedings of the 25th Annual International Conference of the IEEE*, 2003, vol. 1812, p. 1811–1814.

Fish DR, Wingate L. Sources of goniometric error at the elbow. *Phys Ther* 65: 1666–1670, 1985.

Flash T, Mussa-Ivaldi F. Human arm stiffness characteristics during the maintenance of posture. *Exp Brain Res* 82: 315–326, 1990.

Franklin DW, Burdet E, Osu R, Kawato M, Milner TE. Functional significance of stiffness in adaptation of multijoint arm movements to stable and unstable dynamics. *Exp Brain Res* 151: 145–157, 2003.

Franklin DW, Liaw G, Milner TE, Osu R, Burdet E, Kawato M. Endpoint stiffness of the arm is directionally tuned to instability in the environment. *J Neurosci* 27: 7705–7716, 2007.

Franklin DW, Milner TE. Adaptive control of stiffness to stabilize hand position with large loads. *Exp Brain Res* 152: 211–220, 2003.

Gomi H, Osu R. Task-dependent viscoelasticity of human multijoint arm and its spatial characteristics for interaction with environments. *J Neurosci* 18: 8965–8978, 1998.

Gribble PL, Ostry DJ. Independent coactivation of shoulder and elbow muscles. *Exp Brain Res* 123: 355–360, 1998.

Grohmann JE. Comparison of two methods of goniometry. *Phys Ther* 63: 922–925, 1983.

Holzbaur KR, Murray WM, Delp SL. A model of the upper extremity for simulating musculoskeletal surgery and analyzing neuromuscular control. *Ann Biomed Eng* 33: 829–840, 2005.

Hu X, Murray WM, Perreault E. Biomechanical constraints on the control of endpoint stiffness. In: *34th Annual Meeting of American Society of Biomechanics*. Providence, RI: 2010a.

Hu X, Murray WM, Perreault EJ. Modeling the biomechanical constraints on the feedforward control of endpoint stiffness. In: *Engineering in Medicine and Biology Society (EMBC), 2010 Annual International Conference of the IEEE*. 2010b, p. 4498–4501.

Hu X, Murray WM, Perreault EJ. Muscle short-range stiffness can be used to estimate the endpoint stiffness of the human arm. *J Neurophysiol* 105: 1633–1641, 2011.

Hughes R, An K. Monte Carlo simulation of a planar shoulder model. *Med Biol Eng Comput* 35: 544–548, 1997.

Itoi E, Lee SB, Berglund LJ, Schultz FM, Neale PG, An KN. Moment arms of the arm muscles at the glenohumeral joint using the tendon excursion method. *J Musculoskelet Res* 11: 45–53, 2008.

Kadiallah A, Liaw G, Kawato M, Franklin DW, Burdet E. Impedance control is selectively tuned to multiple directions of movement. *J Neurophysiol* 106: 2737–2748, 2011.

Krutky MA, Ravichandran VJ, Trumbower RD, Perreault EJ. Interactions between limb and environmental mechanics influence stretch reflex sensitivity in the human arm. *J Neurophysiol* 103: 429–440, 2010.

Kutch JJ, Valero-Cuevas FJ. Muscle redundancy does not imply robustness to muscle dysfunction. *J Biomech* 44: 1264–1270, 2011.

Lacquaniti F, Carrozzo M, Borghese NA. Time-varying mechanical behavior of multijointed arm in man. *J Neurophysiol* 69: 1443–1464, 1993.

Milner TE. Contribution of geometry and joint stiffness to mechanical stability of the human arm. *Exp Brain Res* 143: 515–519, 2002.

Murray WM, Buchanan TS, Delp SL. Scaling of peak moment arms of elbow muscles with upper extremity bone dimensions. *J Biomech* 35: 19–26, 2002.

Mussa-Ivaldi FA, Hogan N. Integrable solutions of kinematic redundancy via impedance control. *Int J Rob Res* 10: 481–491, 1991.

Mussa-Ivaldi FA, Hogan N, Bizzi E. Neural, mechanical, and geometric factors subserving arm posture in humans. *J Neurosci* 5: 2732–2743, 1985.

Mutha PK, Boulinguez P, Sainburg RL. Visual modulation of proprioceptive reflexes during movement. *Brain Res* 1246: 54–69, 2008.

Ogden C, Fryar C, Carroll M, Flegal K. Mean body weight, height, and body mass index, United States 1960–2002. *Adv Data* 347: 1–17, 2004.

Osu R, Gomi H. Multijoint muscle regulation mechanisms examined by measured human arm stiffness and EMG signals. *J Neurophysiol* 81: 1458–1468, 1999.

Pan P, Peshkin MA, Colgate JE, Lynch KM. Static single-arm force generation with kinematic constraints. *J Neurophysiol* 93: 2752–2765, 2005.

Perreault E, Kirsch R, Crago P. Effects of voluntary force generation on the elastic components of endpoint stiffness. *Exp Brain Res* 141: 312–323, 2001.

Perreault EJ, Kirsch RF, Crago PE. Voluntary control of static endpoint stiffness during force regulation tasks. *J Neurophysiol* 87: 2808–2816, 2002.

Popescu F, Hidler JM, Rymer WZ. Elbow impedance during goal-directed movements. *Exp Brain Res* 152: 17–28, 2003.

Rancourt D, Hogan N. Dynamics of pushing. *J Mot Behav* 33: 351–362, 2001.

Santos V, Valero-Cuevas F. Reported anatomical variability naturally leads to multimodal distributions of Denavit-Hartenberg parameters for the human thumb. *IEEE Trans Biomed Eng* 53: 155–163, 2006.

Selen L, Franklin D, Wolpert D. Impedance control reduces instability that arises from motor noise. *J Neurosci* 29: 12606–12616, 2009.

Tee K, Franklin D, Kawato M, Milner T, Burdet E. Concurrent adaptation of force and impedance in the redundant muscle system. *Biol Cybern* 102: 31–44, 2010.

Tee KP. *Feedback Error Learning at the Muscle Level: A Unified Model of Human Motor Adaptation to Stable and Unstable Dynamics* (Master's thesis). Singapore: National Univ. of Singapore, 2003.

Tee KP, Burdet E, Chew CM, Milner TE. A model of force and impedance in human arm movements. *Biol Cybern* 90: 368–375, 2004.

Trumbower RD, Krutky MA, Yang BS, Perreault EJ. Use of self-selected postures to regulate multi-joint stiffness during unconstrained tasks. *PLoS One* 4: e5411, 2009.

Valero-Cuevas F. A mathematical approach to the mechanical capabilities of limbs and fingers. In: *Progress in Motor Control*. New York: Springer, 2005, p. 619–633.

Yamazaki Y, Suzuki M, Ohkuwa T, Itoh H. Coactivation in arm and shoulder muscles during voluntary fixation of a single joint. *Brain Res Bull* 59: 439–446, 2003.

Zajac FE. Muscle and tendon: properties, models, scaling, and application to biomechanics and motor control. *Crit Rev Biomed Eng* 17: 359–411, 1989.